

## Raman spectroscopy of single nanodiamond: Phonon-confinement effects

K. W. Sun, J. Y. Wang, and T. Y. Ko

Citation: *Applied Physics Letters* **92**, 153115 (2008); doi: 10.1063/1.2912029

View online: <http://dx.doi.org/10.1063/1.2912029>

View Table of Contents: <http://scitation.aip.org/content/aip/journal/apl/92/15?ver=pdfcov>

Published by the [AIP Publishing](#)

---

### Articles you may be interested in

[Phonon screening in photochemically doped zinc oxide nanocrystals](#)

*J. Appl. Phys.* **103**, 074305 (2008); 10.1063/1.2903069

[Micro-Raman spectroscopy of a single freestanding GaN nanorod grown by molecular beam epitaxy](#)

*Appl. Phys. Lett.* **90**, 043102 (2007); 10.1063/1.2433034

[Photoluminescence and multiphonon resonant Raman scattering in low-temperature grown ZnO nanostructures](#)

*Appl. Phys. Lett.* **89**, 071922 (2006); 10.1063/1.2336997

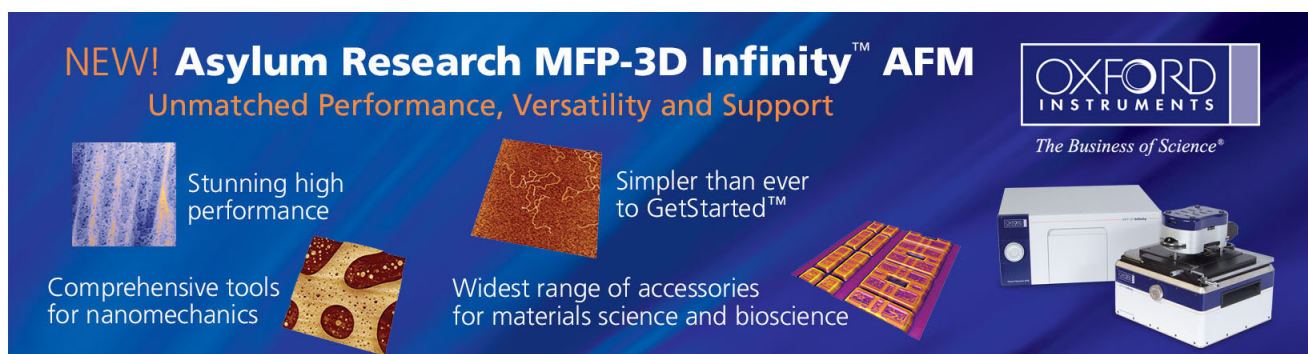
[Raman Spectroscopy of Silicon Nanowires: Phonon Confinement and Anharmonic Phonon Processes](#)

*AIP Conf. Proc.* **685**, 507 (2003); 10.1063/1.1628082

[Phonon confinement effects in the Raman scattering by TiO<sub>2</sub> nanocrystals](#)

*Appl. Phys. Lett.* **72**, 73 (1998); 10.1063/1.120648

---



**NEW! Asylum Research MFP-3D Infinity™ AFM**  
Unmatched Performance, Versatility and Support

**OXFORD INSTRUMENTS**  
*The Business of Science®*

Stunning high performance

Simpler than ever to GetStarted™

Comprehensive tools for nanomechanics

Widest range of accessories for materials science and bioscience

*Asylum Research*

## Raman spectroscopy of single nanodiamond: Phonon-confinement effects

K. W. Sun,<sup>a)</sup> J. Y. Wang, and T. Y. Ko

Department of Applied Chemistry and Institute of Molecular Science, National Chiao Tung University, Hsinchu 300, Taiwan

(Received 23 October 2007; accepted 18 March 2008; published online 17 April 2008)

In this paper, we devise techniques for immobilizing and allocating a single nanodiamond on the electron beam (*e*-beam) patterned smart substrate. The properly designed coordination markers on the semiconductor substrate and the high throughput of the confocal microscope provide us with a convenient tool to single out a nanodiamond with a size less than 100 nm and to study Raman spectroscopy. We observe a redshift in energy and broadening in the linewidth of the  $sp^3$  bonding Raman peak when the size of the diamond is decreased from 90 to 35 nm. The observed shifts and linewidth broadening arise from the phonon-confinement effects and are in good agreement with calculations reported by [Ager *et al.* Phys. Rev. B **43**, 6491 (1991)] and [Yoshikawa *et al.* Appl. Phys. Lett. **62**, 3114 (1993)]. © 2008 American Institute of Physics. [DOI: 10.1063/1.2912029]

In recent years, considerable attention has been focused on the development of techniques for solving applied problems in biology, protein chemistry, molecular biology, etc. In particular, the designs of various biomarker systems based on the Raman and fluorescent properties of nanoparticles hold much promise,<sup>1-5</sup> as opposed to conventional organic fluorophores which suffer from poor photostability, narrow absorption spectra, and broad emission features. Recent advances in the synthesis of the semiconductor nanocrystals have resulted in biomarkers which are brighter, more sensitive, photostable, and biocompatible.<sup>6-8</sup> They have found applications in a variety of biological experiments such as cellular imaging, long-term *in vitro* and *in vivo* labeling, tissue structure mapping, and single-particle investigation of dynamical cellular processes.

More recently, sub-100 nm nanodiamonds with nitrogen point defects have been used as single-particle biomarkers in experiments of fixed and live HeLa cells.<sup>9</sup> It has also been recently demonstrated that diamonds with a nominal size of 100 nm or less are capable of producing stable fluorescence from color centers after surface treatment with strong oxidative acids.<sup>10</sup> The fluorescent nanodiamonds could possibly be used as fluorescent biomarkers for *in vitro* as well as *in vivo* studies at the single-particle level. Although there are some reports on the optical properties of diamond particles, most of the studies focus on diamond particles in clusters or powder form.<sup>11-16,20,21</sup> In this work, we demonstrate phonon properties on a single diamond nanostructure basis by dispersing, immobilizing, and allocating a single nanodiamond on silicon substrates patterned with coordination markers by using (electron beam) lithography techniques. We also report the size effects on the Raman spectra of a single nanodiamond with a confocal microscope.

The methods for dispersing the diamond nanoparticles and the preparation of the patterned smart substrates are given in Ref. 17. A drop of the well diluted nanodiamond solution is placed on the patterned template. After the sample dries out, the surface is scanned by scanning electron microscopy (SEM) to allocate a single nanodiamond. Figure 1(a)

shows the SEM scanning results of two separated single nanodiamonds with sizes of 90 and 35 nm (indicated by the yellow circles in the figure), respectively. Most importantly, from the SEM image, we can ensure that there is no other nanodiamond within the laser focus spot but the selected target before the Raman spectrum measurements. After the target is allocated, their corresponding coordinates are as-

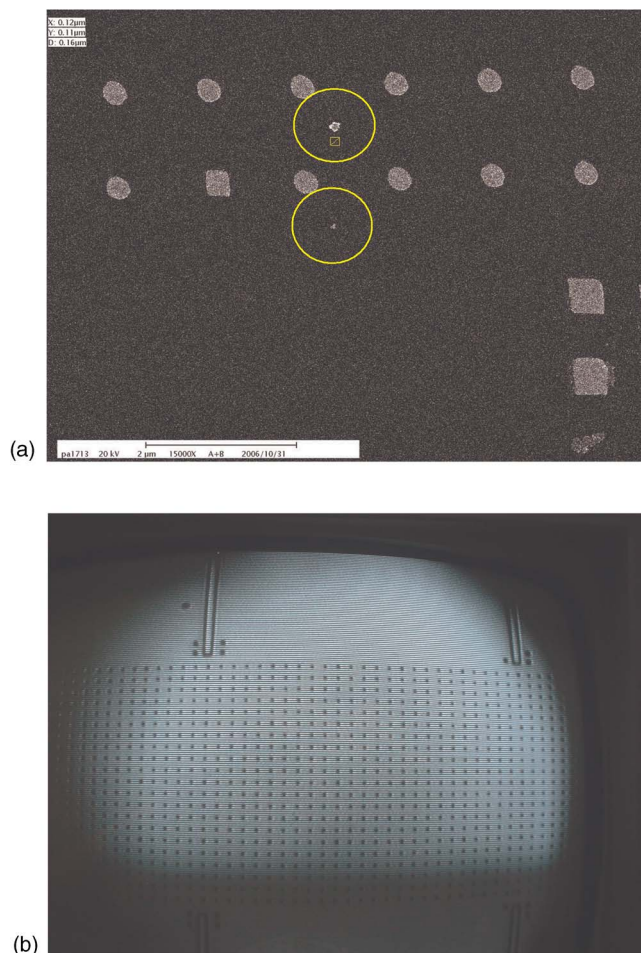


FIG. 1. (Color online) (a) SEM images of the 90 and 35 nm nanodiamonds near the coordination markers. (b) Optical image of the template with the e-beam defined pattern.

<sup>a)</sup> Author to whom correspondence should be addressed. Electronic mail: kwsun@mail.nctu.edu.tw. Tel.: 886 3 571 2121 ext 56581. FAX: 886 3 572 3764.

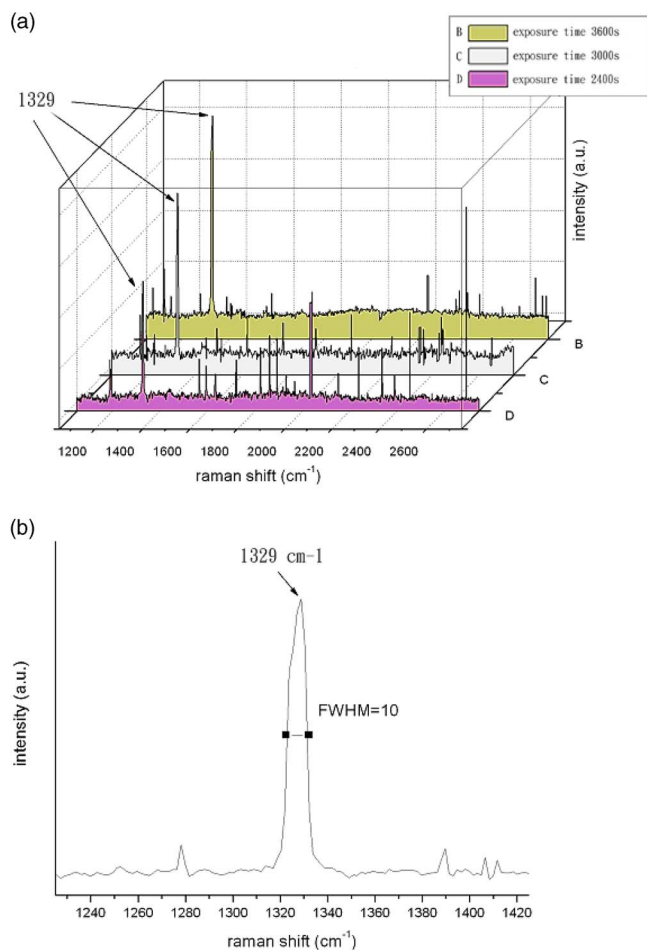


FIG. 2. (Color online) (a) Raman spectra from a single 90 nm diamond with integration time of 2400, 3000, and 3600 s, respectively. (b) Spectrum with improved Signal-to-Noise ratio by averaging spectra in (a). The spectrum shows a single Raman peak at  $1329 \pm 1.5 \text{ cm}^{-1}$  with full width at half maximum of  $10 \text{ cm}^{-1}$ .

signed. Figure 1(b) shows the optical image of the patterned substrate. The dimension of the coordination markers is properly designed so that they can still be clearly seen under the optical microscope. The entire template is moved via an X-Y stepping motor to the given coordinate to position the targets under the laser spot, while the optical image of the substrate is simultaneously monitored on a television screen. The Raman signals are collected through the microscope objective and are analyzed by a 0.32 m spectrometer equipped with a liquid nitrogen cooled charge coupled device-detector at the excitation wavelength of 532 nm. The excitation power density from the diode-pumped solid state laser was controlled under  $10 \text{ KW/cm}^2$  in order not to damage the Si substrates. The optical signal can be further optimized by adjusting the focal plane position along the  $z$  axis via the piezodriven objective lens. The acquired spectra are averaged several times until a good signal-to-noise ratio is achieved.

For the single 90 nm nanodiamond, a Raman peak due to the  $sp^3$  bonding structure in the diamond was detected at the energy of  $1329 \pm 1.5 \text{ cm}^{-1}$  (with a 2400 groove grating) with a linewidth of  $\sim 10 \text{ cm}^{-1}$ , as shown in Fig. 2. This peak is redshifted by  $\sim 3 \text{ cm}^{-1}$  as compared to the bulk diamond. When more than two single nanodiamonds are included within the laser spot, we begin to observe the  $sp^2$  bonding Raman signal at the energy of  $\sim 1600 \text{ cm}^{-1}$  in the spectra

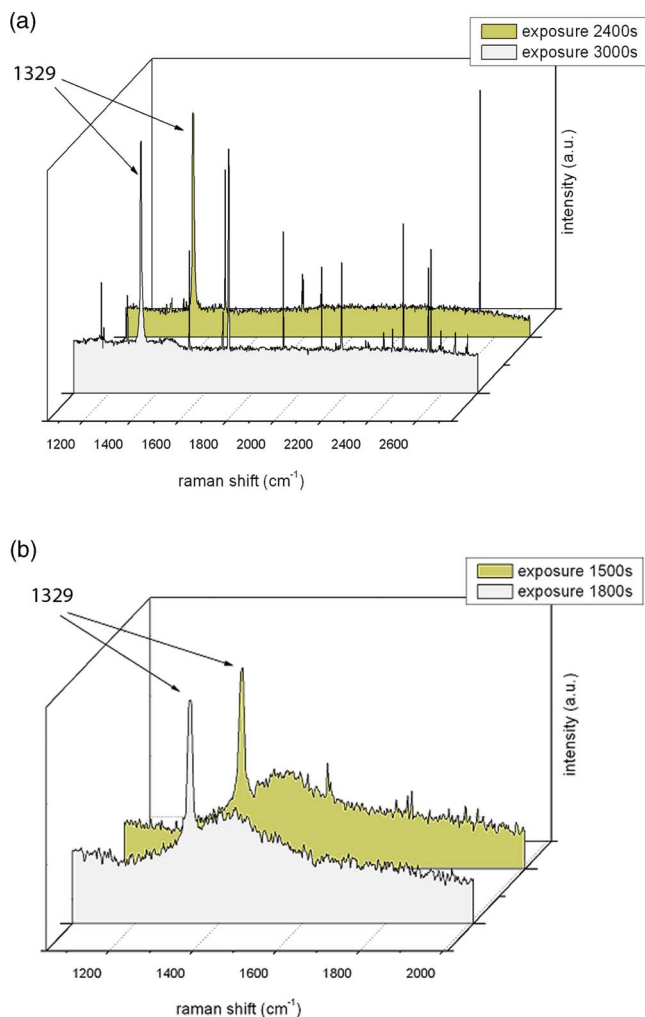


FIG. 3. (Color online) Raman spectra of nanodiamond clusters composed of (a) three and (b) five 90 nm nanodiamonds. The broad peaks near  $1600 \text{ cm}^{-1}$  arise from the  $sp^2$  bonding structure.

shown in Fig. 3. This Raman signal (the  $D$  and  $G$  bands as reported in Ref. 18) originates from a thin graphite layer on the surface of the nanodiamond and is too weak to be detected in the case of a single nanodiamond.

The Raman spectrum from the single 35 nm nanodiamond, as shown in Fig. 4, shows a Raman peak at  $\sim 1325 \pm 1.5 \text{ cm}^{-1}$ . Note that its line shape looks asymmetric and is broadened to  $80 \text{ cm}^{-1}$ . A Raman peak at  $520 \text{ cm}^{-1}$  from the silicon substrate (not shown in the figures) was simultaneously monitored in the measurements. However, we did not observe any shift in energy or change of line shape on this Si Raman peak. The Raman peak intensity also linearly increased with laser power up to 25 mW. Therefore, we concluded that the laser heating or laser-induced thermal effects<sup>19</sup> were insignificant. The Raman spectra were also calibrated by using this Si Raman peak. A strong Raman signature from the  $D$  and  $G$  bands also appears at the energy of  $\sim 1600 \text{ cm}^{-1}$ . Its intensity is comparable to the  $sp^3$  Raman peak, which indicates that this single 35 nm diamond may contain a higher percentage of graphite structure than the 90 nm one.

A theoretical model (known as the phonon-confinement model) was first proposed by Richter *et al.*<sup>20</sup> to explain the observed shift to lower frequency and the broadening of the Raman line in microcrystalline Si. More recently, results of



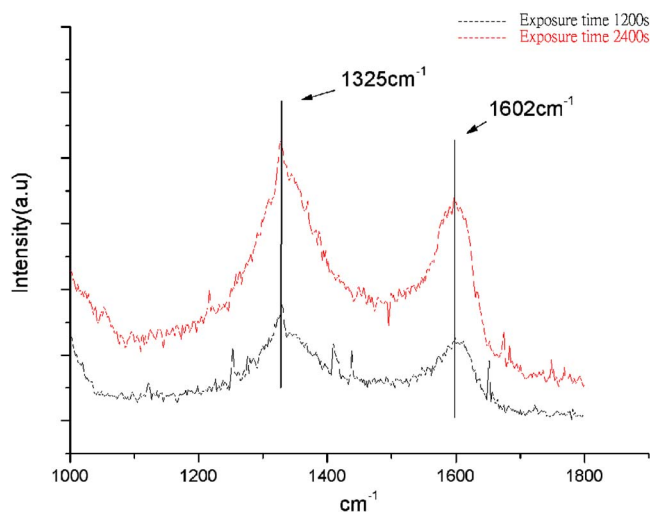


FIG. 4. (Color online) Raman spectra of a single 35 nm diamond with integration times of 2400 and 3600 s, respectively.

phonon-confinement calculations in diamond have been reported in Refs. 15, 21, and 22. The phonon-confinement model is based on the fact that in an infinite crystal, crystal momentum conservation limits Raman spectroscopy to observing phonons at the Brillouin zone center ( $q=0$ ). However, a phonon can be confined in space by microcrystal boundaries in a crystal with finite size. This leads to uncertainty in the phonon momentum which allows phonons with  $q>0$  to contribute to the Raman signal. When the momentum uncertainty is convolved with the dispersion curve, the calculated Raman line shape becomes asymmetrically broadened and the maximum shifts to a lower frequency as the particle size decreases. The calculated results reported by Yoshikawa *et al.*<sup>22</sup> predict that the  $sp^3$  Raman peak shows a redshift of  $\sim 13\text{ cm}^{-1}$  in energy and a linewidth broadening larger than  $50\text{ cm}^{-1}$  as the diamond particle size decreased from 50 to 5 nm. When the confinement length reduced from infinite to 5 nm, an energy shift as large as  $\sim 6\text{ cm}^{-1}$ , asymmetric line shape, and larger broadening of the calculated Raman line were also reported by Ager *et al.*<sup>21</sup>

The linewidth broadening arising from averaging over particles with different sizes can be ruled out because only a single particle is investigated in our studies. The observed energy redshift, change of line shape, and linewidth broadening of the Raman peak in our experiments are attributed to the phonon-confinement effects and are in qualitative agreement with the above theoretical models. The difference in the amount of energy shift and linewidth broadening as compared to the calculations can be explained by the irregular shape of the nanodiamond, which should lead to complications in the calculations, as well as the determination of the true particle size with  $sp^3$  structures.

In summary, by combining a confocal microscope and an e-beam patterned smart substrate, we have been able to study nanodiamond phonon properties on a single nanostructure basis. In contrast to earlier reports on nanodiamond powder or clusters, the factors arising from size distribution can be ruled out and the results can be compared to calculations in parallel. The observed energy redshift and asymmetrical linewidth broadening of the Raman peak in the experiments as the nanoparticle size decreases are attributed to the phonon-confinement effect.

This work was supported by the National Science Council of Republic of China under Contract No. NSC 96-2112-M-009-024-MY3 and the MOE ATU program.

- <sup>1</sup>S. J. Clarke, C. A. Hollmann, Z. Zhang, D. Suffern, S. E. Bradforth, N. M. Dimitrijevic, W. G. Minarik, and J. L. Nadeau, *Nat. Mater.* **5**, 409 (2006).
- <sup>2</sup>I. V. Turchin, I. V. Balalaeva, R. B. Vasil'ev, V. P. Zlomanov, V. I. Plehanov, A. G. Orlova, E. V. Zagaynova, V. A. Kamensky, M. S. Kleshnin, M. V. Shirmanova, S. G. Dorofeev, and D. N. Dirin, *JCT Res.* **3**, 208 (2006).
- <sup>3</sup>A. Fu, W. Gu, C. Larabell, and A. P. Alivisatos, *Curr. Opin. Neurobiol.* **15**, 568 (2005).
- <sup>4</sup>J. Yu, J. Xiao, X. Ren, K. Lao, and X. S. Xie, *Science* **311**, 1600 (2006).
- <sup>5</sup>X. Nan, A. M. Tonary, A. Stolow, X. S. Xie, and J. P. Pezacki, *ChemBioChem* **7**, 1895 (2006).
- <sup>6</sup>X. Michalet, F. Pinaud, T. D. Lacoste, M. Dahan, M. Bruchez, A. P. Alivisatos, and S. Weiss, *Single Mol.* **2**, 261 (2001).
- <sup>7</sup>B. O. Dabbousi, J. Rodriguez-Viejo, F. V. Mikulec, J. R. Heine, H. Mattoussi, R. Ober, K. F. Jensen, and M. J. Bawendi, *J. Phys. Chem. B* **101**, 9463 (1997).
- <sup>8</sup>M. A. Hines and P. J. Guyot-Sionnest, *J. Phys. Chem.* **100**, 468 (1996).
- <sup>9</sup>C.-C. Fu, H.-Y. Lee, K. Chen, T.-S. Lim, H.-Y. Wu, P.-K. Lin, P.-K. Wei, P.-H. Tsao, H.-C. Chang, and W. Fann, *Proc. Natl. Acad. Sci. U.S.A.* **104**, 727 (2007).
- <sup>10</sup>S.-J. Yu, M.-W. Kang, H.-C. Chang, K.-M. Chen, and Y.-C. Yu, *J. Am. Chem. Soc.* **127**, 17604 (2005).
- <sup>11</sup>J. Filik, J. N. Harvey, N. L. Allan, and P. W. May, *Phys. Rev. B* **74**, 035423 (2006).
- <sup>12</sup>F. L. Zhao, Z. Gong, S. D. Liang, N. S. Xu, S. Z. Deng, J. Chen, and H. Z. Wang, *Appl. Phys. Lett.* **85**, 914 (2004).
- <sup>13</sup>J. Chen, S. Z. Deng, J. Chen, Z. X. Yu, and N. S. Xu, *Appl. Phys. Lett.* **74**, 3651 (1999).
- <sup>14</sup>M. E. Kompan, E. I. Terukov, S. K. Gordeev, and S. G. Zhukov, *Phys. Solid State* **39**, 1928 (1997).
- <sup>15</sup>M. Yoshikawa, Y. Mori, H. Obata, M. Maegawa, G. Katagiri, H. Ishida, and A. Ishitani, *Appl. Phys. Lett.* **67**, 694 (1995).
- <sup>16</sup>Y. Namba, E. Heidarpour, and M. J. Nakayama, *Appl. Phys. A* **72**, 1748 (1992).
- <sup>17</sup>See EPAPS Document No. E-APPLAB-92-041816, for the methods of dispersing the diamond nanoparticles and the preparation of the patterned smart substrates. For more information of EPAPS, see <http://www.aip.org/epaps/numbering.html>.
- <sup>18</sup>M. Yoshikawa, N. Nagai, M. Matsuki, H. Fukuda, G. Katagiri, H. Ishida, and A. Ishitani, *Phys. Rev. B* **46**, 7169 (1992).
- <sup>19</sup>J. E. Spanier, R. D. Robison, F. Zhang, S.-W. Chan, and I. P. Herman, *Phys. Rev. B* **64**, 245407 (2001).
- <sup>20</sup>H. Richer, Z. P. Wang, and L. Ley, *Solid State Commun.* **39**, 625 (1981).
- <sup>21</sup>J. W. Ager III, D. Kirk Veirs, and G. M. Rosenblatt, *Phys. Rev. B* **43**, 6491 (1991).
- <sup>22</sup>M. Yoshikawa, Y. Mori, M. Maegawa, G. Katagiri, H. Ishida, and A. Ishitani, *Appl. Phys. Lett.* **62**, 3114 (1993).